Article

Research on Coal Gangue Recognition Based on Multi-source Time−Frequency Domain Feature Fusion

Yao Zhang,[†] Yang Yang,*,[†] and Qingliang Zeng*
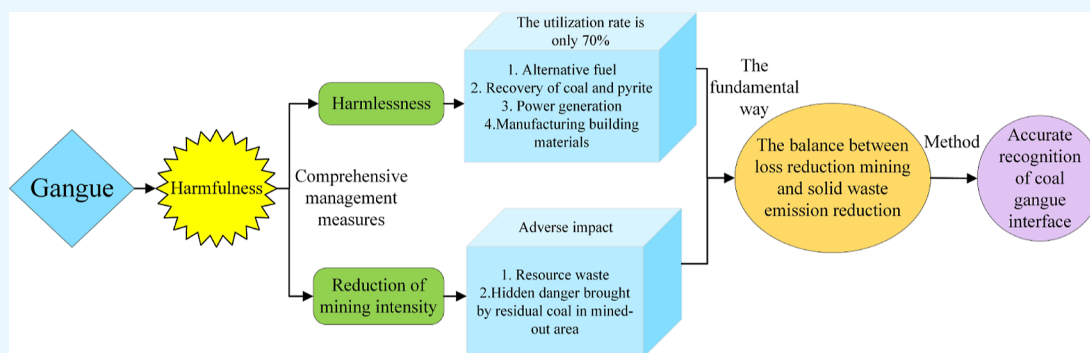
Cite This: ACS Omega 2023, 8, 25221−25235

Read Online

ACCESS | ░░ Metrics & More | ▣ Article Recommendations

ABSTRACT: The over-exploitation of resources caused by the increasing coal demand has resulted in a sharp increase in solid waste emissions mainly gangue, which has made the burden on the environment, economy, resources, and society of our country heavier. In order to achieve a balance between energy consumption and solid waste emission in the process of top coal caving, this study carried out coal gangue recognition research based on multi-source time−frequency domain feature fusion (MS-TFDF-F). First, the process of coal gangue symbiosis and the harm of gangue in top coal caving are analyzed, and the fundamental method of comprehensive treatment of gangue is put forward, which is the accurate recognition of the coal gangue interface. Second, by building a top coal caving simulation test bed, the MS signals generated in the caving process of the coal gangue mixture with a gangue content of 0−100% are collected and the TFDFs are extracted. Third, the MS-TFDF-F-based coal gangue recognition model is established. Then, the recognition effect of the two TFDF-F sample sets was compared, and the results show that the time−frequency domain feature selection fusion method (TFDFS-FM) has higher accuracy. On this basis, this paper studies the variation law of the number of sensors on the coal gangue recognition accuracy of MS information fusion. Finally, the economic, social, environmental, and resource benefits of the model are qualitatively described. The final results show that the MS-TFDF-F-based coal gangue recognition model has the strongest recognition ability when fusing six sensor signals, and the recognition accuracy reaches 99% under the AdaBoost algorithm. The establishment of this model brings huge benefits to China's environment, economy, resources, and society, and it is helpful to realize the balance between loss reduction mining and solid waste emission reduction in the process of top coal caving.

1. INTRODUCTION

Coal is the cornerstone of China's energy security. Because of its abundant reserves and wide distribution compared with other energy sources, it plays an extremely important role in the development of China's society, economy, and other aspects.[1] Top coal caving is an efficient mining method suitable for the thick and extra-thick coal seams in China.[2,3] At present, the development status of the industry is high mining intensity and low caving technology level, resulting in a high gangue rate, which imposes additional burdens on the environment, economy, and other aspects. Under the background of China's carbon peaking and carbon neutrality goals,[4] it is of extreme significance to realize clean coal production by strengthening scientific and technological support.

Gangue is a common solid waste in the process of geological mineral mining.[5,6] In the actual coal production process, coal and gangue coexist symbiotically. With the support and encouragement of relevant policies and mechanisms, there are more and more ways of comprehensive utilization of coal gangue, such as recycling useful minerals,[7] gangue for power generation,[8] sintering into useful materials,[9,10] grouting
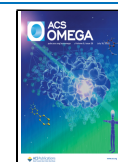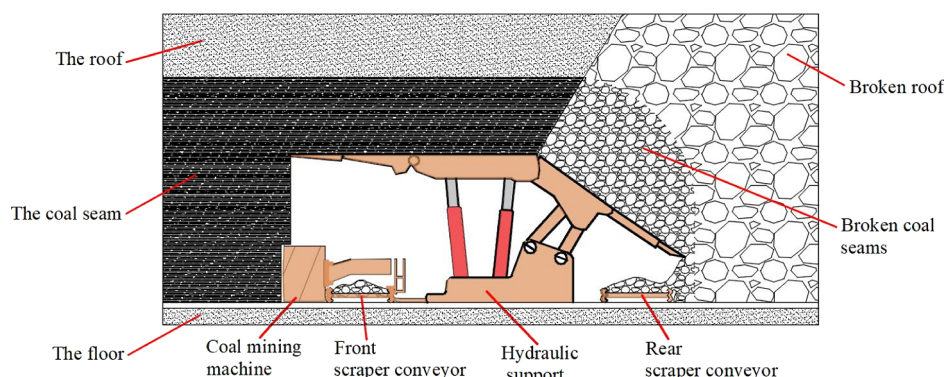
Figure 1. Schematic diagram of top coal caving.

filling,[11,12] etc. However, the volume of gangue and its harm under long-term accumulation should not be underestimated, especially in the area with a low utilization rate of gangue in western China. Therefore, while ensuring the coal recovery rate, technical research should be strengthened to make the gangue emissions reach the standard. At present, the widely used artificial coal gangue interface discrimination method is easy to cause misjudgment. Accurate and reliable coal gangue recognition technology is the fundamental way to solve this problem.

In order to realize the balance between loss reduction mining and solid waste emission reduction in top coal caving, this study establishes an MS-TFDF-F-based coal gangue recognition model, which can accurately judge the coal gangue interface and improve the recognition accuracy. The model is expected to control the generation of gangue from the source and achieve clean coal production.

Many studies have been carried out based on image,[13−16] vibration,[17−19] sound,[20−22] γ rays,[23,24] Lidar,[25,26] and other media. Recently, Wang et al.[27] proposed a semantic segmentation network for coal gangue image recognition. Li et al.[28] innovatively uses the density characteristics of coal and gangue for recognition. Zhang et al.[29] makes the thermal infrared images of coal and gangue more significant through the intervention of different liquids. Wang et al.[30] established a coal gangue recognition model based on dielectric parameters and geometric characteristic parameters of coal and gangue. In the early stages, aiming at the problem of low recognition accuracy of single-source multi-point vibration acceleration signals, our team carried out a study on coal gangue recognition based on time-domain feature cross-optimal fusion, and the recognition accuracy finally reached 97%.[31]

To sum up, most of the existing studies are based on different single properties of coal and gangue, while there are few studies on MS information fusion generated by a variety of different properties of coal gangue. Due to the differences in various properties of coal and gangue in different mining areas, it is easy to lead to the problems of insufficient recognition accuracy and weak generalization ability of the coal gangue recognition model established based on a single information source. In addition, current research lacks the screening of the location and type of sensors, which is limited by the availability of sensor data and the discriminability of recognition features.[32] In addition, only the time domain features were cross-optimal selected, and the feature selection method needs to be further improved.

In view of the gaps and shortcomings of previous studies, this paper will simultaneously screen the sensors and TFDFs of signals based on the fusion of MS signals and TFDFs. The purpose is to increase the effective information as well as reducing the amount of computation, so as to further improve the recognition accuracy. The innovations in this study are as follows.

(1) The fundamental method of comprehensive treatment of gangue is explored.
(2) Two feature fusion methods, OTFDF-FM and TFDFS-FM, are proposed and compared.
(3) The MSI-FM based on vibration signals, pressure signals, and acoustic signals is proposed.
(4) The MS-TFDF-F-based coal gangue recognition model is established.
(5) The fusion frequency of each feature in the process of TFDFS-FM is studied.
(6) The benefits of the MS-TFDF-F-based coal gangue recognition model are qualitatively analyzed.

The specific work route of this paper is as follows. Section 2 discusses the process of top coal caving and the harm of gangue and explores the ways of comprehensive treatment of gangue. Section 3 extracts MS signals of top coal caving through experiments and establishes a MS-TFDF-F-based coal gangue recognition model. Section 4 verifies the performance of the coal gangue recognition model under the AdaBoost algorithm. Section 5 qualitatively analyzes the benefits of the model. Section 6 shows the relevant conclusions.

2. MODEL BUILDING BACKGROUND

Under the pressure of increasing energy demand in China, the problem of solid waste discharge caused by the excessive strength of coal mining is becoming increasingly difficult to solve. This section introduces the process of top coal caving and the harm of gangue and explores the fundamental way of comprehensive treatment of gangue.

2.1. Introduction of Top Coal Caving Process. Fully mechanized top coal caving is one of the main mining methods suitable for thick and extra-thick coal seam mining in China, which has many advantages such as low cost, low tunneling rate, high recovery rate, and strong adaptability.[33,34]

The coal seam generally occurs in the coal-bearing rock formation, located between the roof and floor strata. With the advancement of coal mining at the working face, the coal seam floor plays a supporting role, and the roof is above the coal seam. With the mining of the whole roadway coal seam, the roof fall fills the mined-out area. In some mining areas, the
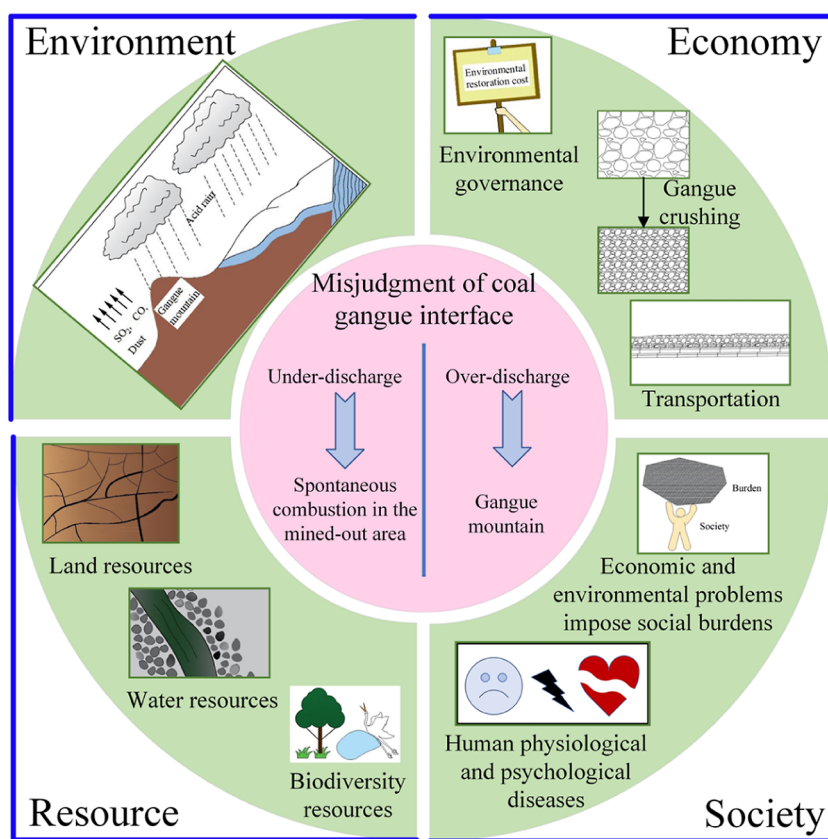
Figure 2. Hazards of gangue.

coal−rock interface is not obvious due to geological processes, and the closer the coal seam is to the roof, the higher the gangue content is.

As shown in Figure 1, the front scraper conveyor transfers the coal from the shearer to the coal face. Meanwhile, the hydraulic support supports the upper coal seam. Then, the hydraulic support moves forward, and the upper coal seam is induced to collapse, falling onto the unfolded tail beam and the extended insert plate.[35−37] Then the hydraulic control system controls the tail beam to open and the insert plate to recover. The broken coal falls from the coal caving port and is transported out of the mining working face by the rear scraper conveyor. When the gangue content in the fallen coal reaches the shutdown threshold, the hydraulic system is timely controlled to close the tail beam and extend the insert plate to prevent a large amount of gangue from further falling out with the coal flow.

2.2. Hazards of Gangue. At present, mine workers determine the coal gangue interface by auditory and visual inspection. The influence of subjective consciousness and the noise and the dark environment of the mine often lead to misjudgment, resulting in over-discharge or under-discharge. If over-discharging, a large amount of gangue will be transported out of the working face with coal flow, and if under-discharging, a large amount of coal will be left in the mined-out area, which is easy to cause spontaneous combustion[38,39] and gas explosion.[40−42] In the context of China's current energy mining, top coal over-discharge occurs from time to time, and a large amount of gangue mining ground has a serious impact on China's environment, economy, other resources and society,[43−45] as shown in Figure 2.

(1) Impact on the environment

Gangue is a kind of industrial waste containing many harmful components. Because the use of gangue has not been fully developed, it is difficult to achieve industrialization and often accumulates near the mining area. A large number of harmful gases, such as SO_2 and CO, are produced by the spontaneous combustion of heat accumulated inside the gangue dumped into the atmospheric environment, forming acid rain. In addition, a large amount of dust produced by the disintegration and weathering of gangue has a bad impact on the mining area's environment.

(2) Impact on the economy

The impact of gangue on the economy is mainly reflected in the following three aspects. (a) The extra cost of coal transportation, coal washing, and gangue crushing in the process of gangue production. (b) The accumulation of gangue mountains occupies land, resulting in the loss of cultivated land resources and affecting the development of the agricultural economy. (c) Environmental degradation will generate most of the economic expenditure on environmental remediation.

(3) Impact on other resources

The gangue mined with coal will occupy and destroy land resources. With the intensification of coal mining, the occupation of land resources by gangue becomes more and more serious. Harmful elements in gangue dissolve in water and penetrate into the soil, resulting in water destruction, excessive heavy metals, soil fertility decline, etc. The destruction of the atmospheric environment, land resources, and water resources in coal mining areas will lead to an imbalance of the ecological environment, a change in plant
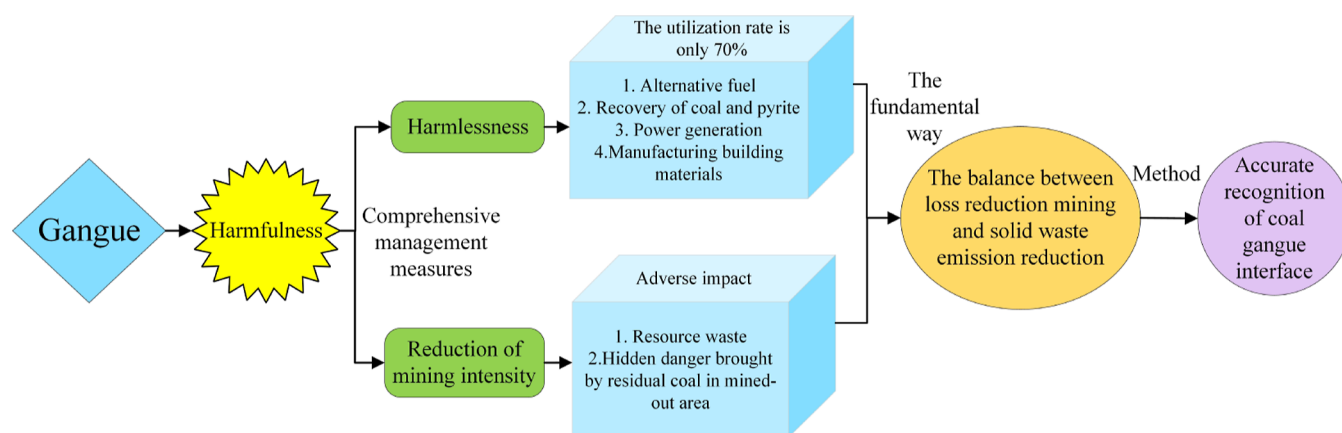
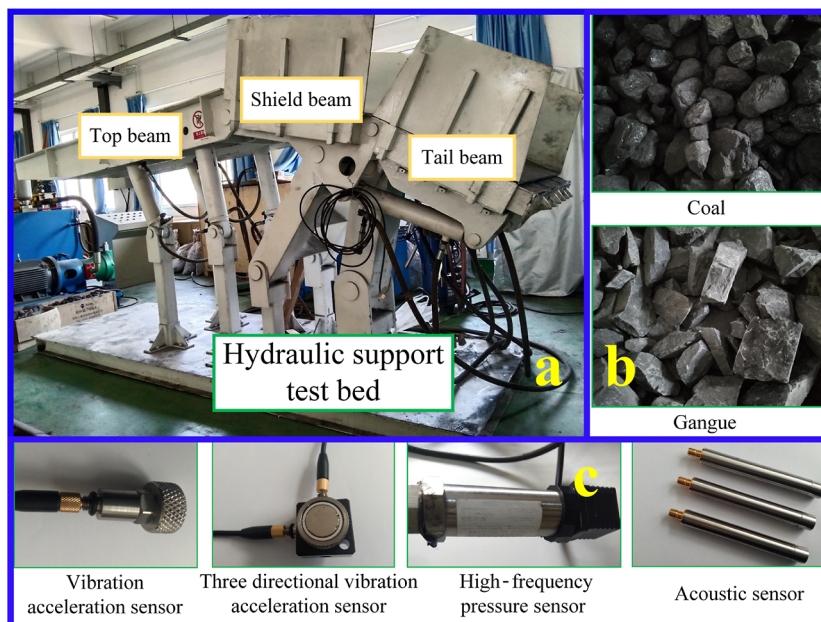**Figure 3.** Comprehensive treatment method of gangue.

Figure 4. Test bed. (a) Test bed physical prototype. (b) Coal and gangue for test. (c) Signal acquisition equipment.

growth conditions, the destruction of animal habitat, and then the loss of biodiversity resources.

(4) Impact on society

The environmental and economic impacts caused by gangue will inevitably lead to a series of negative social effects. Human and material resources will be spent on environmental remediation, while the population will be more likely to suffer from physical and mental illness.

2.3. Fundamental Treatment Method of Gangue. Gangue is the solid waste produced in the process of coal mining and coal washing and transported to the ground with coal. An excessive coal recovery rate will inevitably cause a large number of gangue output. The treatment of gangue can be carried out in two aspects: recycling (harmless) and reducing mining. For the recovery and utilization of gangue, its use mainly includes replacing fuel, recycling coal and pyrite, power generation, manufacturing building materials, etc. Although China has extended the industrial chain of gangue in many aspects to make it a valuable resource for reuse, it is still unable to realize its industrialization, with the utilization rate only reaching more than 70%. If the gangue is not mined,

it will not cause great harm to all aspects of society. If the mining intensity is reduced in order to reduce the gangue content, it may cause the top coal to be under-discharged. Coal flows into the mined-out area with gangue, resulting in a waste of resources and even the hidden danger of spontaneous combustion. Solving the problem of gangue content while greatly reducing the output of resources will be more than worth the loss.
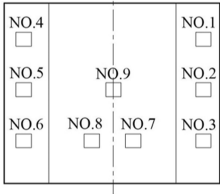
While meeting the national standard of gangue rate, improving the coal recovery rate is the best coal mining goal. Therefore, achieving the balance between loss reduction mining and solid waste emission reduction in top caving coal is the fundamental way of comprehensive treatment of gangue, and the accurate recognition technology of the coal gangue interface is the fundamental method to solve this problem. The comprehensive treatment approach for coal gangue is shown in Figure 3.

3. TEST AND DATA PROCESSING

In order to improve the accurate perception ability of the coal gangue recognition model at the coal gangue interface, this

Table 1. Location of the MS Signal Sensors

Sensors	Sensor number	Installation location
Vibration acceleration sensor at the bottom of tail beam	NO.1	Schematic diagram of the sensors installation on the bottom of the tail beam
	NO.2	
	NO.3	
	NO.4	NO.4 □ NO.1 □
	NO.5	NO.5 □ NO.9 □ NO.2 □
	NO.6	NO.6 □ NO.8 □ NO.7 □ NO.3 □
	NO.7	
	NO.8	
	NO.9	
Axis pin vibration acceleration sensor	NO.10	Installed on the outer end face axis of the pin connecting the cover beam to the tail beam on the left side of the hydraulic support through the magnetic suction base
	NO.11	
High frequency pressure sensor	NO.12	Installed on the bottom end of two tail beam jacks by threaded connection
	NO.13	
Acoustic sensor	NO.14	Under the tail beam
	NO.15	Under the shield beam
	NO.16	At the junction of the tail beam and the shield beam on the left side of the hydraulic support

study integrates vibration, pressure, and acoustic sensors to collect MS information on coal and gangue. The methods of time domain, frequency domain, and time−frequency domain fusion are used to process MS information data.

3.1. Top Coal Caving Test. As shown in Figure 4, the test bed is an in-lab impact slip test bed transformed with reference to ZF5600 hydraulic support for top coal caving so as to imitate the actual top coal caving working surface. The coal gangue mixture with different mixing ratios slides from the shield beam and impacts the tail beam. In this process, the signal acquisition system collects MS signals.

The signal acquisition system mainly includes four parts: MS signal sensors (9 sets of 1A102E universal piezoelectric vibration acceleration sensors, 1 set of 1A302E three directional vibration acceleration sensor, 2 sets of CYB41 high-frequency pressure sensors, and 3 sets of MPA426 acoustic sensors), constant voltage power supply for sensor power supply, dynamic signal test and analysis system for signal transmission, and DHDAS dynamic signal analysis system for signal storage. At the same time, noise reduction and anti-mixing filtering modules are added to the data acquisition system. The test also performs noise reduction filtering on the signal from both software and hardware. In the software part, the noise reduction program is added to the data acquisition process according to the Butterworth low-pass filtering principle, and the principle of the Faraday cage is applied to electrostatic shielding in the hardware part. The location of the MS signal sensors is shown in Table 1.

During the test, the coal gangue mixed sample is dumped on top of the shield beam, slides down to the upper surface of the tail beam to produce certain impact vibrations and sounds, and changes the oil pressure of the tail beam jack. The sampling frequency is set to 10,000 Hz, and the MS signals collected by each sensor are transmitted to the DHDAS dynamic signal analysis system for storage by the DH8302 and DH5925 dynamic signal test and analysis system. 16 MS signals obtained from each set of coal gangue mixed sample tests are stored in a folder. Table 2 shows the number of test groups

conducted for coal gangue mixed samples with different gangue mixing rates.

Table 2. Number of Samples with Different Gangue Mixing Rates

mixed gangue rate (%)	0	0−5	5−10	10−15	15−20
number of samples	30	22	47	72	74
mixed gangue rate (%)	20−25	25−30	30−40	40−50	50−60
number of samples	853	995	40	11	11
mixed gangue rate (%)	60−70	70−80	80−90	90−100	100
number of samples	10	10	10	9	29

A total of 2223 groups of tests were carried out in this study. According to the requirements of relevant regulations on top coal caving, this paper takes the gangue ratio of 25% as the classification threshold, and defines the samples with a gangue ratio of less than 25% as the "caving category", with a total of 1098 groups, and the samples with a ganging ratio greater than 25% were defined as the "shutdown category", totaling 1125 groups.

3.2. MS Information Data Processing. In this section, all signals collected during the test are preprocessed as follows. The first data point that is 0.25 m/s^2 greater than the acceleration at the initial time is taken as the first data point and the effective time domain length is set to 2.5 s. Each signal is a standardized time−acceleration signal with a length of 25,001 after preprocessing, as shown in Figure 5.

Then, each signal is processed in the time domain and the frequency domain, respectively. Time domain processing refers to the direct extraction of 12 features such as mean, absolute mean, and standard deviation for standardized signals. Frequency domain processing refers to the extraction of 12 features such as spectrum mean, frequency variance, and frequency center of gravity for the signals after fast Fourier transform,[46−48] as shown in Figure 6. The feature expression is shown in Table 3.
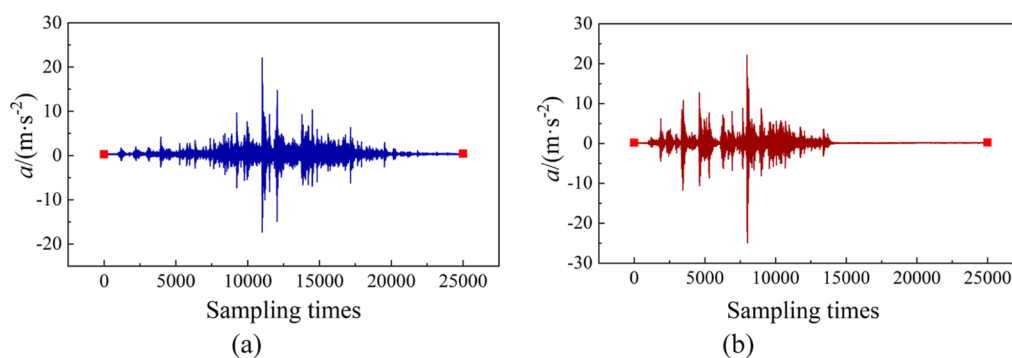
Figure 5. Time domain signal waveform diagram. (a) Coal and (b) gangue.
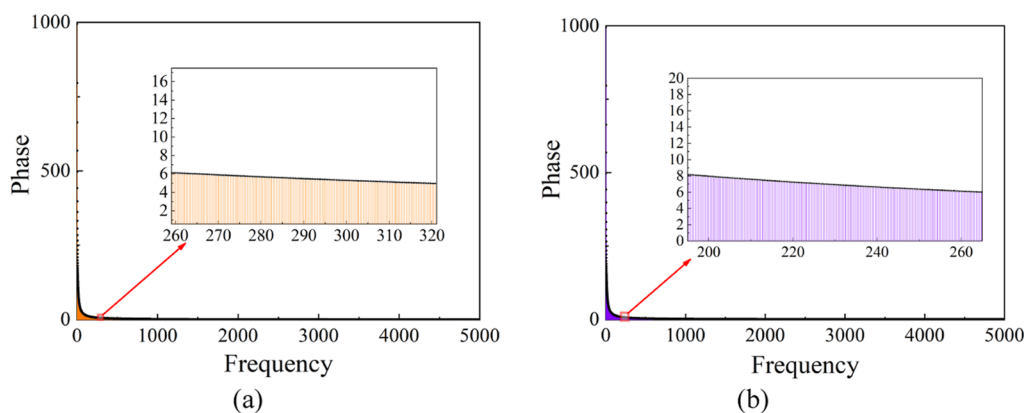

Figure 6. Frequency domain signal waveform diagram. (a) Coal and (b) gangue.

4. MODEL ESTABLISHMENT AND VERIFICATION

In the previous section, we collected the vibration acceleration signals of the bottom of the tail beam, the bidirectional vibration acceleration signals of the pin shaft, the high-frequency pressure signals, and the acoustic signals around the test bed during the coal gangue impact test and extracted the time domain and frequency domain features of each signal. On this basis, this section will carry out the study of coal gangue recognition based on MS-TFDF-F, as shown in Figure 7.

First, this paper proposes two TFDF-F methods. The first one is the overall time−frequency domain feature fusion method (OTFDF-FM). In this method, the time domain features and frequency domain features of the same signal are connected in series to form a coal gangue recognition eigenmatrix containing all signal features. Then, to simplify the recognition model and improve the recognition accuracy, the time−frequency domain feature selection fusion method (TFDFS-FM) is proposed. The first six features with the highest recognition accuracy among all time domain and frequency domain features are retained, and various combinations of them are traversed. The optimal feature subset is the feature combination with the highest recognition accuracy, which is the result of TFDF-F. The pseudocode of TFDFS-FM is shown in Figure 8.

Second, in order to increase the effective information and reduce the computational complexity, the MS information fusion method (MSI-FM) is proposed. On the basis of the two kinds of TFDF-F methods, the better one is selected for MS information fusion. The specific fusion steps are as follows. The recognition accuracy of 16 sensors was sorted, and the sensor signals were selected for parallel fusion according to the recognition accuracy from high to low. One sensor was selected each time for a total of 16 fusions, and the optimal sensor combination with the highest recognition accuracy was selected. According to the principle of selecting a small number of sensors with the same recognition accuracy, the final MS-TFDF-F result is obtained.

Finally, the MS-TFDF-F-based coal gangue recognition model is established based on the above research, and the recognition process is shown in Figure 9. First, each signal collected by the sensors is processed to extract 12 time domain features and 12 frequency domain features. Second, according to the boundary of 25% gangue content, it is divided into two kinds of coal gangue recognition sample sets: "caving category" and "shutdown category". Then, 400 groups of samples are randomly selected from the "caving category" and "shutdown category" sample sets as the training set and 200 groups of samples are randomly selected as the test set, respectively. Finally, the training set and the test set are input into the MS-TFDF-F-based coal gangue recognition model, and the recognition accuracy of the sample set is obtained. The time domain and frequency domain feature fusion method is selected according to the recognition results, and the recognition accuracy of each sensor is sorted based on the selected fusion method. The sensors are selected successively for parallel combination, and finally trained into a MS-TFDF-F-based coal gangue recognition model with the highest recognition accuracy.

5. RESULTS AND DISCUSSION

In this section, the AdaBoost recognition algorithm[49−51] is used to recognize the MS-TFDF-F sample sets of coal gangue and the performance of the recognition model is verified. The

Table 3. Time Domain and Frequency Domain Feature Expressions[a]

serial number	time domain features	serial number	frequency domain features
1	$F_{td1} = \dfrac{1}{n}\sum_{i=1}^{n} x(i)$	13	$F_{fd1} = \dfrac{1}{K}\sum_{k=1}^{K} s(k)$
2	$F_{td2} = \dfrac{1}{n}\sum_{i=1}^{n} |x(i)|$	14	$F_{fd2} = \dfrac{1}{K}\sum_{k=1}^{K} [s(k)]^2$
3	$F_{td3} = \sqrt{\dfrac{1}{n}\sum_{i=1}^{n} [x(i) - F_{td1}]^2}$	15	$F_{fd3} = \dfrac{\sqrt{k-1}\sum_{k=1}^{K} [s(k) - F_{fd1}]^3}{[\sum_{k=1}^{K} [s(k) - F_{fd1}]^2]^{3/2}}$
4	$F_{td4} = \left(\dfrac{1}{n}\sum_{i=1}^{n} \sqrt{|x(i)|}\right)^2$	16	$F_{fd4} = \dfrac{(K-1)\sum_{k=1}^{K} [s(k) - F_{fd1}]^4}{[\sum_{k=1}^{K} [s(k) - F_{fd1}]^2]^2}$
5	$F_{td5} = \sqrt{\dfrac{1}{n}\sum_{i=1}^{n} [x(i)]^2}$	17	$F_{fd5} = \dfrac{\sum_{k=1}^{K} f_k \cdot s(k)}{\sum_{k=1}^{K} s(k)}$
6	$F_{td6} = \max[x(i)] - \min[x(i)]$	18	$F_{fd6} = \sqrt{\dfrac{1}{K-1}\sum_{k=1}^{K} (f_k - F_{fd5})^2 \cdot s(k)}$
7	$F_{td7} = \dfrac{\frac{1}{n}\sum_{i=1}^{n} (x_i - F_{td1})^3}{\left[\frac{1}{n}\sum_{i=1}^{n} (x_i - F_{td1})^2\right]^{3/2}}$	19	$F_{fd7} = \sqrt{\dfrac{\sum_{k=1}^{K} f_k^2 \cdot s(k)}{\sum_{k=1}^{K} s(k)}}$
8	$F_{td8} = \dfrac{|\max[x(i)]|}{\frac{1}{n}\sum_{i=1}^{n} |x(i)|}$	20	$F_{fd8} = \sqrt{\dfrac{\sum_{k=1}^{K} f_k^4 \cdot s(k)}{\sum_{k=1}^{K} f_k^2 \cdot s(k)}}$
9	$F_{td9} = \dfrac{\frac{1}{n}\sum_{i=1}^{n} (x_i - F_{td1})^4}{\left[\frac{1}{n}\sum_{i=1}^{n} (x_i - F_{td1})^2\right]^2}$	21	$F_{fd9} = \dfrac{\sum_{k=1}^{K} f_k^2 \cdot s(k)}{\sqrt{\sum_{k=1}^{K} s(k)\sum_{k=1}^{K} f_k^4 \cdot s(k)}}$
10	$F_{td10} = \dfrac{\max|x(i)|}{\left(\frac{1}{n}\sum_{i=1}^{n} \sqrt{|x(i)|}\right)^2}$	22	$F_{fd10} = \dfrac{F_{fd6}}{F_{fd5}}$
11	$F_{td11} = \dfrac{|\max[x(i)]|}{\sqrt{\frac{1}{n}\sum_{i=1}^{n} [x(i)]^2}}$	23	$F_{fd11} = \dfrac{\sum_{k=1}^{K} (f_k - F_{fd5})^3 \cdot s(k)}{(K-1)F_{fd6}^3}$
12	$F_{td12} = \dfrac{\sqrt{\frac{1}{n}\sum_{i=1}^{n} [x(i)^2]}}{\frac{1}{n}\sum_{i=1}^{n} |x(i)|}$	24	$F_{fd12} = \dfrac{\sum_{k=1}^{K} (f_k - F_{fd5})^4 \cdot s(k)}{(K-1)F_{fd6}^4}$

[a]Here, $n = 25{,}001$ and $x(i)$ is the value of the corresponding vibration signal acceleration at the ith ($1 \leq i \leq 25{,}001$) sampling point. $s(k)$ is the spectrum of the signal $x(i)$ and f_k is the frequency value of the kth spectral line. ($k = 1, 2, ..., K$. K is the number of spectral lines).

algorithm sets consistent frame parameters, as shown in Table 4.

5.1. Recognition Results of OTFDF-FM. First, we analyze the recognition results of the OTFDF-FM. Table 5 shows recognition results under the AdaBoost algorithm for the sample set of time domain, frequency domain, and TFDF-F of each sensor signal and all sensor parallel signals.

As shown in Table 5, the recognition accuracy of the TFDF-F is slightly higher than the time domain and frequency domain features for most single sensors. When all sensor signals are used in parallel, the recognition result of TFDF-F is lower than that of time domain features.

It can be seen from Figure 10 that on the whole, the recognition result of signal TFDF-F is the best, followed by the frequency domain feature, and the time domain feature is the worst. Whether in time domain feature, frequency domain feature, or TFDF-F, the recognition accuracy of all sensor signals in parallel is higher than that of each single sensor. The highest recognition accuracy of signal TFDF-F only reaches 97%, which is lower than the highest recognition accuracy of

time domain features of 97.3%. Therefore, the OTFDF-FM is not effective in improving recognition accuracy.

5.2. Recognition Results of TFDFS-FM. Recognition results of the OTFDF-FM are analyzed in this section. Table 6 shows the recognition results and fused features under the AdaBoost algorithm for the sample set of time domain, frequency domain, and TFDF-F of each sensor signal and all sensor parallel signals. To ensure the comparability of recognition results, we perform feature selection according to the same principle for time domain and frequency domain features. That is, the first six features with the highest recognition accuracy are retained, and their various combinations are traversed to find the optimal feature subset and obtain the recognition results.

The fused feature subset in Table 6 is the feature combination with the highest recognition accuracy. Therefore, the stronger the classification ability of the feature for the target task, the higher the possibility that it will be retained. In order to explore the classification ability of each time domain and frequency domain feature, we made statistics on the frequency of features in the process of time domain, frequency
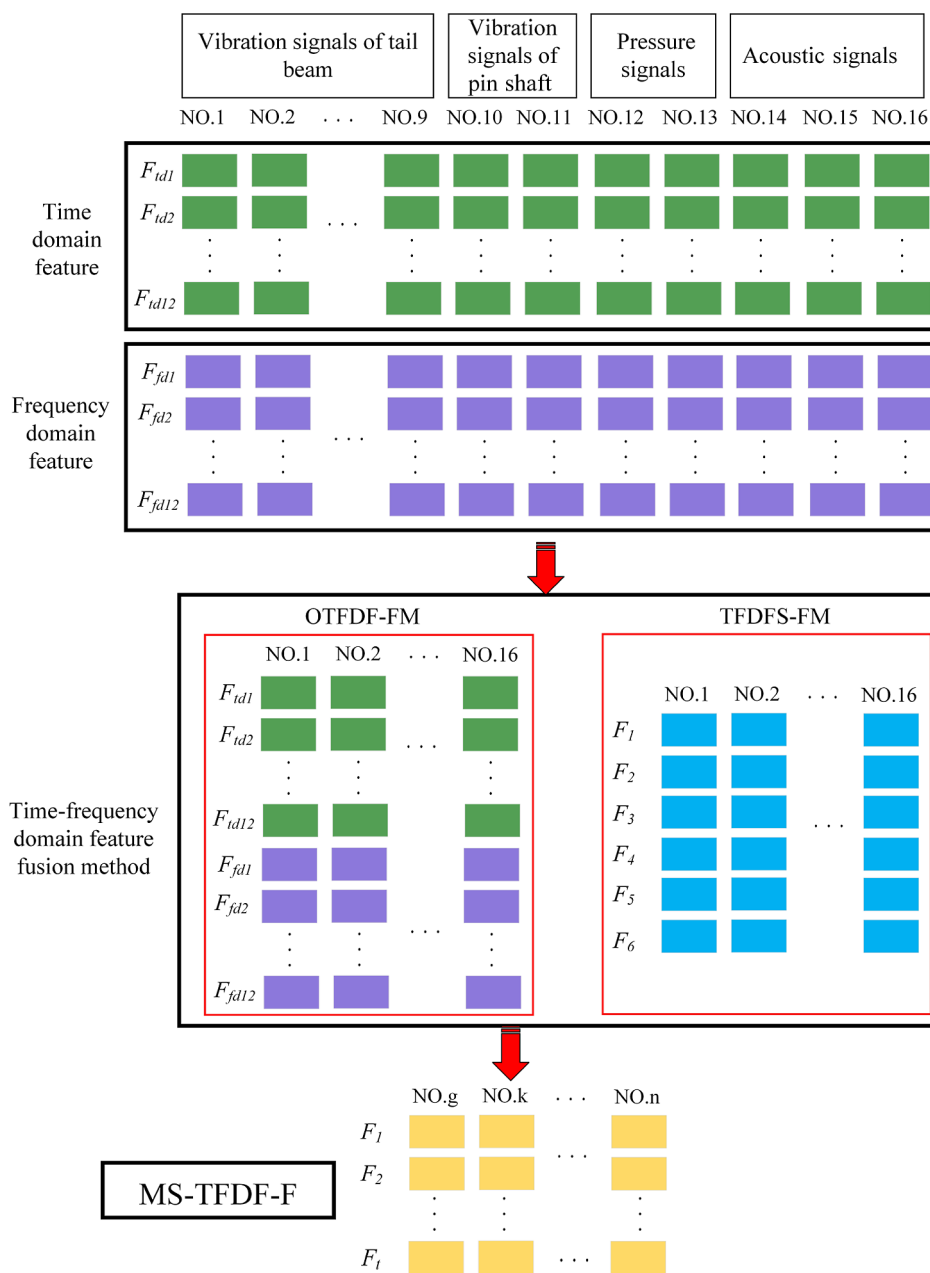
Figure 7. Diagram of the MS-TFDF-F process.

domain, and TFDF-F-based selection fusion, as shown in Table 7.

As shown in Table 7, the feature with the highest frequency is F_{td1}, which appears 24 times in total and has a strong classification sensitivity for the signal sample. The lowest frequency features are F_{td7} and F_{td12}, which did not play a role in this recognition experiment based on the TFDFS-FM.

Figure 11 shows the frequency of time domain and frequency domain features in the recognition experiment based on feature selection fusion, respectively. It can be seen from the figure that the overall sensitivity of frequency domain features is higher than that of time domain features. The frequency of each feature is sorted, and the result is as follows.

$$F_{td1} > F_{fd7} > F_{td4} = F_{fd5} > F_{fd9} > F_{fd6} > F_{fd11}$$
$$> F_{td2} = F_{td3} = F_{fd12} > F_{fd3} = F_{fd8}$$
$$> F_{td5} = F_{fd2}$$

$$> F_{fd1} = F_{fd10} > F_{td11} > F_{td10}$$
$$> F_{td8} = F_{td9} = F_{fd4} > F_{td7} > F_{td12}$$

According to Table 6, we compare the recognition accuracy of the time domain, frequency domain, and time−frequency domain features of each sensor signal based on the TFDFS-FM, as shown in Figure 12.

According to Figure 12, the recognition accuracy of TFDF-F is significantly higher than that of time domain features and frequency domain features under the TFDFS-FM. Recognition results of 16 sensor signals connected in parallel are distinctly higher than those of each single sensor, and the highest

Algorithm: Principle of the TFDFS-FM

input: Training set
input: Test set
input: F_{tdi}: Time domain features, F_{fdj}: Frequency domain features
1　　$M \leftarrow [\ ]$
2　　**for** features in F_{tdi}, F_{fdj} **do**
3　　　$model1.fit$ (Training set)
4　　　$AC \leftarrow model1.score$ (Test set)
5　　　$M.append(AC)$
6　　**end**
7　　$N \leftarrow$ The top six features with the highest accuracy
8　　$Q \leftarrow$ Generate all feature subsets of N
9　　$E \leftarrow [\ ]$
10　**for** j in Q **do**
11　　$model2.fit$ (Training set)
12　　$ACC \leftarrow model2.score$ (Test set)
13　　$E.append(ACC)$
14　**end**
15　$n \leftarrow E.argmax(\ )$
16　**output:** $Q[n], E[n] \leftarrow$ The result of MS-TFDF-F

Figure 8. Pseudocode of the TFDFS-FM.

recognition accuracy is 98.8% after TFDF selection fusion. The TFDFS-FM has an obvious effect on improving recognition accuracy.

5.3. Comparison of Recognition Accuracy of Two Feature Fusion Methods. Above, we compare the recognition results before and after the fusion of the two TFDF-F methods. According to Tables 5 and 6, this section will compare the two feature fusion methods. First, the recognition results of all features and feature selection in time domain and frequency domain are compared, as shown in Figure 13a,b, respectively.

As shown in Figure 13a, the recognition accuracy of time domain feature selection is higher than that of all time domain features under most sensors. As shown in Figure 13b, the recognition accuracy of frequency domain feature selection and all frequency domain features varies from sensor to sensor. Then, we compare the recognition accuracy of the two methods of OTFDF-FM and TFDFS-FM, as shown in Figure 14.

As shown in Figure 14, the recognition accuracy of the TFDFS-FM is higher than that of the OTFDF-FM under most sensors by comparing the recognition accuracy. In general, the recognition results of the TFDFS-FM are better, and this feature selection method can reduce the number of classification features to 6 or less, which is less than the 24

Table 4. Definition of AdaBoost Classifier System and Parameters

parameters	definition	implication
n_estimators	20	the number of weak learners
algorithm	SAMME.R	the prediction probability of sample set fraction is used as the weight of weak learner
learning_rate	1	weight reduction coefficient of weak learner
base_estimator	AdaBoostClassifier	the weak learner is the classification learner

Table 5. Recognition Results Based on OTFDF-FM

	sensor number	time domain	frequency domain	time−frequency domain
vibration acceleration sensor at the bottom of tail beam	NO.1	0.713	0.860	0.853
	NO.2	0.733	0.770	0.790
	NO.3	0.863	0.825	0.910
	NO.4	0.658	0.733	0.753
	NO.5	0.790	0.778	0.835
	NO.6	0835	0.850	0.873
	NO.7	0.710	0.778	0.775
	NO.8	0.690	0.735	0.733
	NO.9	0.748	0.765	0.775
axis pin vibration acceleration sensor	NO.10	0.800	0.768	0.783
	NO.11	0.790	0.778	0.780
high frequency pressure sensor	NO.12	0.840	0.890	0.895
	NO.13	0.728	0.853	0.900
acoustic sensor	NO.14	0.698	0.785	0.795
	NO.15	0.743	0.770	0.798
	NO.16	0.818	0.888	0.878
ALL		0.973	0.965	0.970

inherent features in the OTFDF-FM, greatly reducing the computational complexity of the model. Therefore, the following research is based on the TFDFS-FM.

5.4. Analysis of the Recognition Results of Each Single Sensor. In this section, the recognition accuracy of each single sensor is analyzed based on the TFDFS-FM. Table 8 and Figure 15 shows the recognition accuracy of each single sensor.

As shown in Table 8 and Figure 15, the recognition accuracy varies greatly among the nine vibration acceleration sensors at
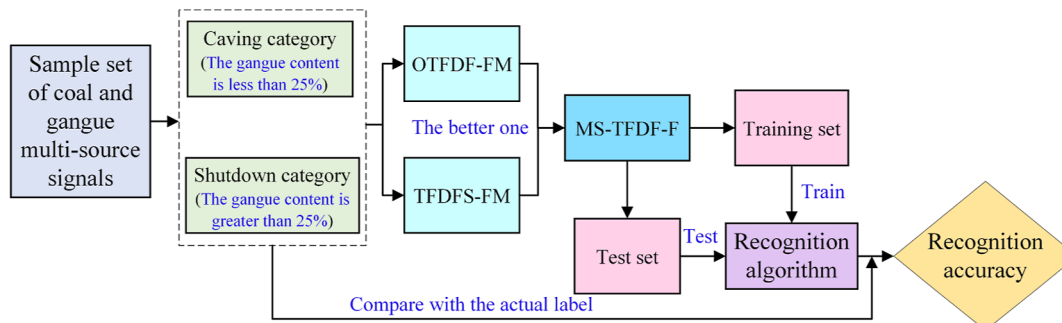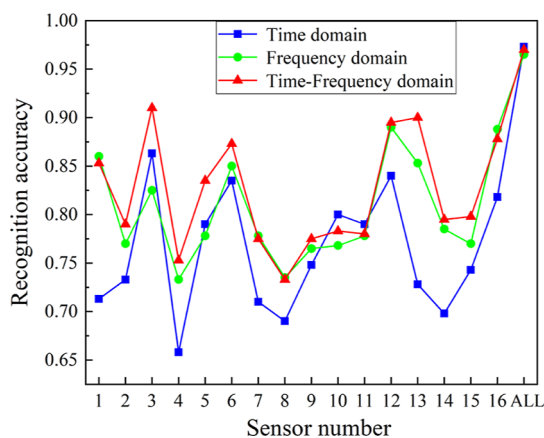

Figure 9. MS-TFDF-F-based coal gangue recognition model.

Figure 10. Comparison of recognition results based on the OTFDF-FM.

the bottom of the tail beam. Although several groups of sensors are in mutually symmetric positions, the symmetry of the recognition accuracy is also extremely unobvious, which is caused by the uneven position of the gangue particles sliding. Therefore, the sensitivity cannot be defined only based on the sensor position. The recognition accuracy of the axis pin vibration sensor has no obvious advantage compared with other sensors, and the recognition accuracy of the acceleration signal generated by the x-direction vibration is higher than that generated by the y-direction vibration. The recognition accuracy of the signals detected by the two pressure sensors is high. The recognition accuracy of acoustic sensors varies depending on the sensor position. The recognition accuracies of single sensor signals are sorted as follows.

$$\text{NO. 3} = \text{NO. 13} > \text{NO. 16} > \text{NO. 1} > \text{NO. 12}$$
$$> \text{NO. 6} > \text{NO. 5} > \text{NO. 7} > \text{NO. 10} > \text{NO. 15}$$
$$> \text{NO. 2} > \text{NO. 9} = \text{NO. 11} = \text{NO. 14} > \text{NO. 4}$$
$$> \text{NO. 8}$$

5.5. Coal Gangue Recognition Results Based on MS Time−Frequency Feature Fusion. Based on the TFDFS-FM with better results and the recognition accuracy ranking of each single sensor, we carry out the recognition research of MS information fusion in this section. Sensors are selected for MS information fusion according to the recognition accuracy of the single sensor TFDF-F from high to low. The relationship between the number of fusion sensors and the recognition accuracy as well as the fusion features is shown in the following table.

According to Table 9, the frequency of each time domain and frequency domain feature in the process of MS information fusion is counted, as shown in Table 10. (Only the features appearing in the process of MS information fusion are counted.)

The feature with the highest frequency is F_{td1}, which appears 16 times in total, followed by F_{fd10}, which appears 12 times in total.

According to Figure 16, the frequency of each feature is sorted.

$$F_{td1} > F_{fd10} > F_{td2} > F_{td3} > F_{td4} = F_{fd3} > F_{fd5}$$
$$> F_{fd4} = F_{fd6} = F_{fd7} = F_{fd8}$$

Table 6. Recognition Results Based on TFDFS-FM

	time domain	frequency domain	time−frequency domain
	recognition results and the fused features	recognition results and the fused features	Recognition results and the fused features
NO.1	0.765	0.853	0.893
	$[F_{td1}, F_{td4}]$	$[F_{fd6}, F_{fd11}]$	$[F_{td1}, F_{fd5}, F_{fd8}, F_{fd11}]$
NO.2	0.753	0.783	0.803
	$[F_{td1}, F_{td5}]$	$[F_{fd6}, F_{fd7}, F_{fd11}]$	$[F_{td1}, F_{fd7}]$
NO.3	0.873	0.828	0.918
	$[F_{td1}, F_{td5}]$	$[F_{fd6}, F_{fd7}, F_{fd8}, F_{fd11}, F_{fd12}]$	$[F_{td1}, F_{fd3}, F_{fd7}, F_{fd8}]$
NO.4	0.713	0.775	0.758
	$[F_{td1}, F_{td3}, F_{td4}, F_{td5}]$	$[F_{fd5}, F_{fd7}, F_{fd12}]$	$[F_{fd5}, F_{fd7}, F_{fd9}, F_{fd11}]$
NO.5	0.803	0.793	0.863
	$[F_{td1}, F_{td4}]$	$[F_{fd2}, F_{fd5}]$	$[F_{td1}, F_{fd8}, F_{fd9}]$
NO.6	0.858	0.838	0.880
	$[F_{td1}, F_{td3}, F_{td4}, F_{td5}]$	$[F_{fd6}, F_{fd7}, F_{fd9}, F_{fd11}, F_{fd12}]$	$[F_{fd5}, F_{fd7}, F_{fd8}, F_{fd9}]$
NO.7	0.758	0.788	0.830
	$[F_{td1}, F_{td3}]$	$[F_{fd6}, F_{fd7}, F_{fd11}, F_{fd12}]$	$[F_{td1}, F_{fd7}, F_{fd9}]$
NO.8	0.723	0.773	0.745
	$[F_{td1}, F_{td11}]$	$[F_{fd5}, F_{fd7}, F_{fd9}, F_{fd12}]$	$[F_{fd5}, F_{fd12}]$
NO.9	0.773	0.773	0.780
	$[F_{td1}, F_{td3}, F_{td4}]$	$[F_{fd2}, F_{fd6}, F_{fd9}]$	$[F_{td1}, F_{fd6}, F_{fd9}, F_{fd12}]$
NO.10	0.808	0.775	0.825
	$[F_{td1}, F_{td3}, F_{td4}]$	$[F_{fd1}, F_{fd2}, F_{fd7}]$	$[F_{td1}, F_{td4}, F_{fd9}]$
NO.11	0.790	0.785	0.780
	$[F_{td1}, F_{td2}]$	$[F_{fd5}, F_{fd7}, F_{fd9}, F_{fd12}]$	$[F_{td2}, F_{td4}, F_{fd5}, F_{fd7}]$
NO.12	0.855	0.855	0.885
	$[F_{td1}, F_{td2}, F_{td3}, F_{td4}, F_{td5}, F_{td10}]$	$[F_{fd3}, F_{fd6}, F_{fd10}]$	$[F_{fd1}, F_{fd3}]$
NO.13	0.735	0.855	0.918
	$[F_{td1}, F_{td2}, F_{td3}]$	$[F_{fd5}, F_{fd7}, F_{fd9}, F_{fd12}]$	$[F_{td1}, F_{fd1}, F_{fd2}, F_{fd3}]$
NO.14	0.713	0.755	0.780
	$[F_{td1}, F_{td2}, F_{td3}, F_{td4}]$	$[F_{fd5}, F_{fd7}]$	$[F_{td2}, F_{td4}, F_{fd6}, F_{fd11}]$
NO.15	0.735	0.818	0.818
	$[F_{td6}, F_{td8}, F_{td11}]$	$[F_{fd5}, F_{fd8}, F_{fd11}]$	$[F_{fd5}, F_{fd7}]$
NO.16	0.785	0.878	0.898
	$[F_{td2}, F_{td4}, F_{fd9}, F_{td10}]$	$[F_{fd2}, F_{fd5}, F_{fd10}]$	$[F_{td2}, F_{td4}, F_{fd5}, F_{fd9}, F_{fd10}]$
ALL	0.983	0.978	0.988
	$[F_{td1}, F_{td4}, F_{td11}]$	$[F_{fd3}, F_{fd6}, F_{fd9}]$	$[F_{td1}, F_{td2}, F_{fd3}, F_{fd10}]$

The ranking of feature frequency and its sensitivity are different by comparing Table 7 with Table 10, which proves that the classification ability of features varies greatly with different data sets. Therefore, in practical applications, it is not only necessary to perform a simple series fusion of all features but also to screen out the most useful feature subset for the corresponding sample set classification.

According to Table 9, the following figure shows our graph of the recognition accuracy as a function of the number of sensors fused in the process of MS information fusion.

As shown in Figure 17, the highest recognition accuracy is achieved when the number of fused sensors is in the interval of 6−11. When the recognition accuracy is consistent, we try to select a smaller number of sensors for fusion so as to reduce the computational pressure of data processing and learning.

Table 7. Statistics of Feature Frequency

| features	F_{td1}	F_{td2}	F_{td3}	F_{td4}	F_{td5}	F_{td6}	F_{td7}	F_{td8}	F_{td9}	F_{td10}	F_{td11}	F_{td12}
frequency	24	9	9	14	5	1	0	1	1	2	3	0
features	F_{fd1}	F_{fd2}	F_{fd3}	F_{fd4}	F_{fd5}	F_{fd6}	F_{fd7}	F_{fd8}	F_{fd9}	F_{fd10}	F_{fd11}	F_{fd12}
frequency	4	5	6	1	14	11	16	6	12	4	10	9

(a) (b)
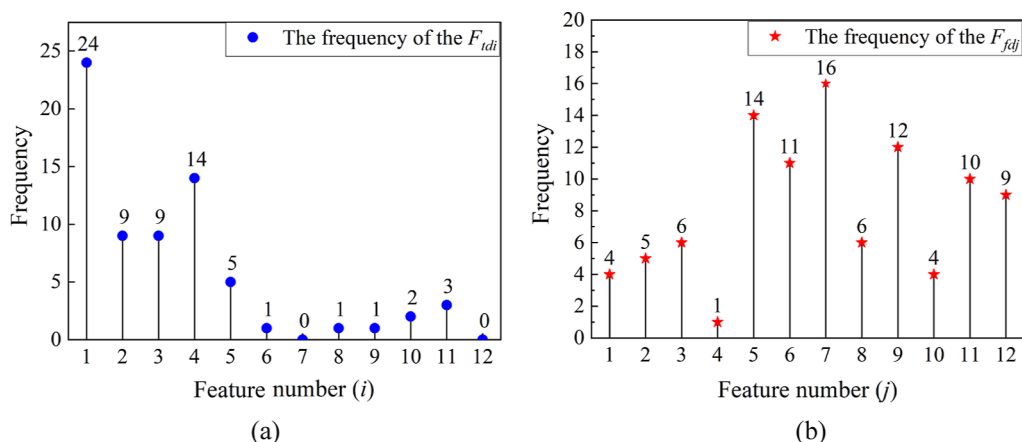
Figure 11. Frequency of features. (a) Frequency of each time domain feature in the feature selection fusion process. (b) Frequency of each frequency domain feature in the feature selection fusion process.
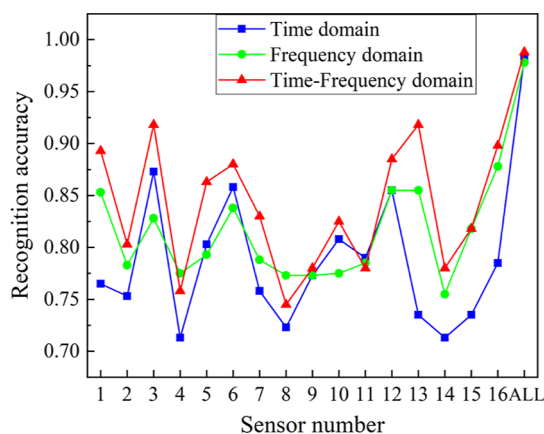
Figure 12. Comparison of recognition results based on the TFDFS-FM.
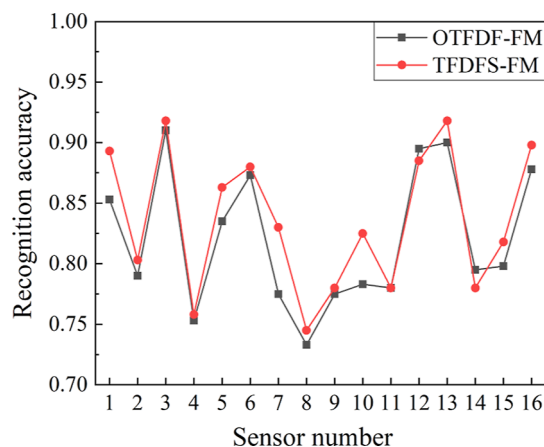
**Figure 14.** Comparison of time−frequency domain fusion recognition results of two feature selection methods.

(a) (b)
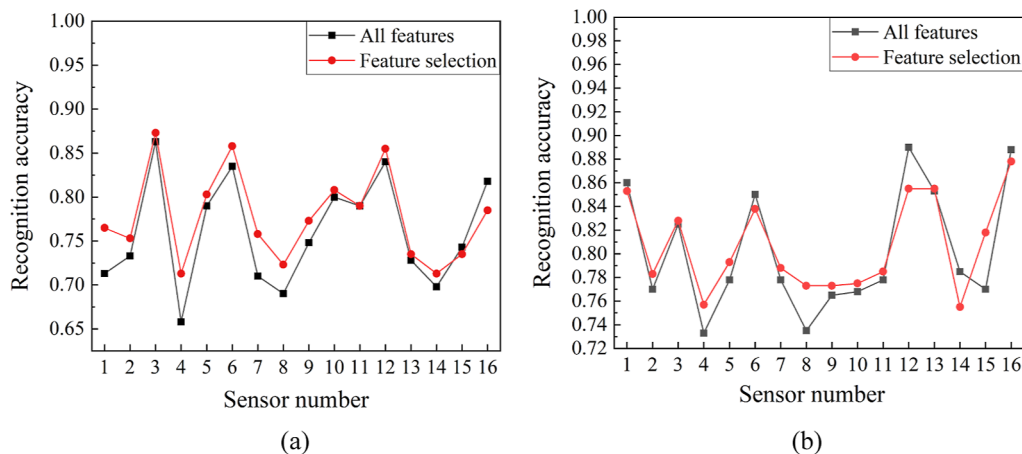
Figure 13. Comparison of recognition results of all features and feature selection. (a) Comparison of recognition results of two feature selection methods in the time domain. (b) Comparison of recognition results of two feature selection methods in the frequency domain.

Table 8. Recognition Accuracy of Each Single Sensor

| sensor number	NO.1	NO.2	NO.3	NO.4	NO.5	NO.6	NO.7	NO.8
recognition accuracy	0.893	0.803	0.918	0.758	0.863	0.880	0.830	0.745
sensor number	NO.9	NO.10	NO.11	NO.12	NO.13	NO.14	NO.15	NO.16
recognition accuracy	0.780	0.825	0.780	0.885	0.918	0.780	0.818	0.898
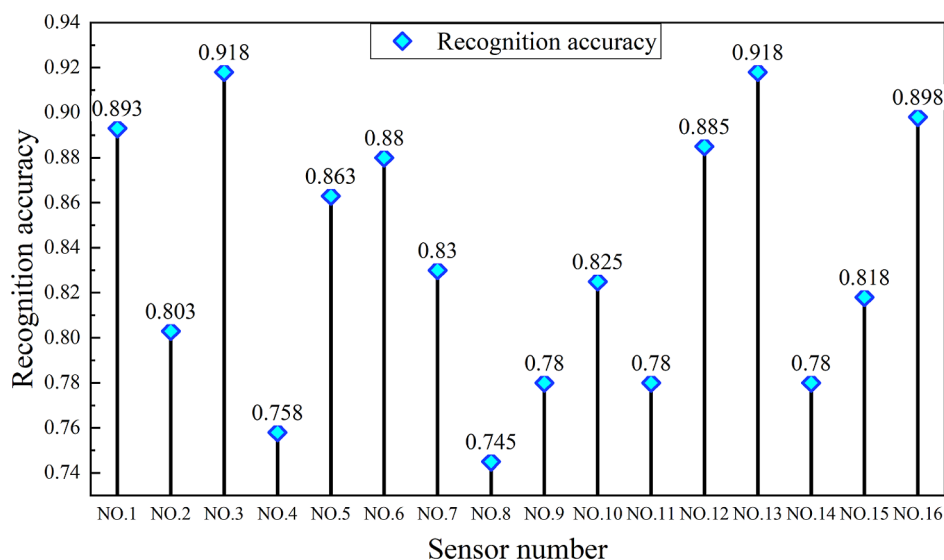
Figure 15. The recognition accuracy of each single sensor based on the TFDFS-FM.

**Table 9. Recognition Results and Fusion Features of MS-TFDF-F**

number of sensors	1	2	3	4
recognition results and the fused features	0.918	0.965	0.988	0.983
	$[F_{td1}, F_{fd3}, F_{fd7}, F_{fd8}]$	$[F_{td1}, F_{fd3}, F_{fd4}, F_{fd5}]$	$[F_{td1}, F_{fd3}, F_{fd10}]$	$[F_{td1}, F_{fd3}, F_{fd5}]$
number of sensors	5	6	7	8
recognition results and the fused features	0.983	0.99	0.99	0.99
	$[F_{td1}, F_{fd3}, F_{td4}, F_{fd10}]$	$[F_{td1}, F_{td2}, F_{td3}, F_{td4}, F_{td6}]$	$[F_{td1}, F_{td2}, F_{td3}, F_{fd10}]$	$[F_{td1}, F_{td4}, F_{fd10}]$
number of sensors	9	10	11	12
recognition results and the fused features	0.99	0.99	0.99	0.988
	$[F_{td1}, F_{td2}, F_{fd10}]$	$[F_{td1}, F_{td2}, F_{fd10}]$	$[F_{td1}, F_{td2}, F_{fd10}]$	$[F_{td1}, F_{td4}, F_{fd10}]$
number of sensors	13	14	15	16
recognition results and the fused features	0.988	0.988	0.988	0.988
	$[F_{td1}, F_{td2}, F_{td3}, F_{fd10}]$	$[F_{td1}, F_{td2}, F_{td3}, F_{fd10}]$	$[F_{td1}, F_{td2}, F_{td3}, F_{fd10}]$	$[F_{td1}, F_{td2}, F_{td3}, F_{fd10}]$

Table 10. Statistics of Feature Frequency

features	F_{td1}	F_{td2}	F_{td3}	F_{td4}	F_{fd3}	F_{fd4}	F_{fd5}	F_{fd6}	F_{fd7}	F_{fd8}	F_{fd10}
frequency	16	9	7	4	4	1	2	1	1	1	12
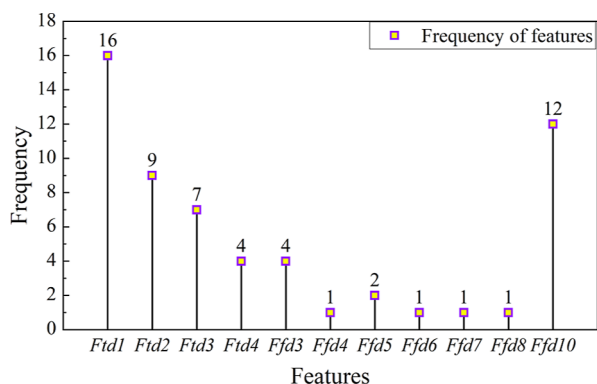
Figure 16. Frequency of features.
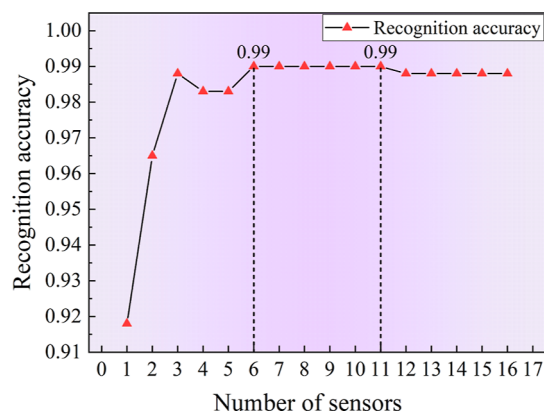
Figure 17. Recognition results based on the MS-TFDF-F.

Finally, the number of fusion sensors in the MS-TFDF-F-based coal gangue recognition model is six, and the recognition accuracy reaches 99%. Six sensors are numbered NO.3, NO.13, NO.16, NO.1, NO.12, and NO.6, a fusion of three vibration acceleration sensors, two high-frequency pressure sensors, and one acoustic sensor.

6. APPLICATION ANALYSIS

China's coal demand is a large and growing trend, mainly used in thermal power generation, industrial boilers, domestic coal, and other aspects. Although the output of gangue in the process of coal mining will cause harm to the environment, economy, resources, and society, the characteristics of "rich coal, poor oil, and less gas" in the energy structure of China determine that coal will continue to occupy the main body of energy in our country, so the growth trend of it will not change significantly in the short term. The following will qualitatively analyze the benefits of various aspects of the coal gangue recognition model.

For the environment and green sustainable development, the application of coal gangue recognition intelligent technology can not only reduce the impact of gangue on the environment but also avoid the spontaneous combustion of residual coal in the mined-out area and the harmful gas pollution of the environment, which is conducive to the green sustainable development of coal mine production.

In terms of economy, each ton of gangue needs to consume transportation and lifting costs of about 14.26 yuan, and the cost of moving the sieve of 2.25 yuan. In addition, there are coal washing costs, evaluation costs, depreciation costs, and the impact of gangue on coal quality costs. The cost of producing one ton of gangue in China is 89.54 yuan through comprehensive calculation, so reducing the output of gangue can greatly reduce the cost of coal mining. In addition, it also reduces the input of environmental governance costs.

In terms of resources, the accurate recognition of the coal gangue interface avoids the situation of under-discharging and over-discharging, reduces the consumption of land, water, biology, and other resources by solid waste emission, and realizes loss reduction mining to increase the output of coal resources as much as possible. China's raw coal production has been on the rise every year since 2016. According to the current coal mining technology in China, 14 million tons of gangue will be discharged for every 100 million tons of coal produced. At present, more than 3 billion tons of gangue are stored in China, covering about 12,000 hectares. Governance of gangue is conducive to promoting the liberation of cultivated land in China.

In recent years, China has issued a series of policies on coal mining, supporting the coal industry to develop in the direction of intelligence and efficiency, which will also promote the further development of coal mining. In addition, as an irreplaceable fuel and raw material for power, steel, building materials, and chemical industries, the overall development trend of coal in the future is stable growth. Under the background of national advocacy for green mining, it is of profound significance to achieve a balance between loss reduction mining and solid waste emission reduction.

The establishment of the MS-TFDF-F-based coal gangue recognition model and the wide application of this technology will bring great benefits to China's environment, economy, resources, and society, as summarized in Table 11.

Table 11. Benefits Analysis of the Recognition Model

	benefits
environment	(1) the harm of gangue output to atmosphere, water source, and soil is reduced
	(2) the risk of a large number of harmful gases produced by spontaneous combustion in mined-out area is reduced
	(3) it promotes the green and sustainable development of the local ecological environment
economy	(1) the extra cost of gangue production, transportation, and crushing is reduced
	(2) the cost of environmental remediation caused by gangue treatment is avoided
	(3) make full use of the economic benefits brought by coal resources
resources	(1) it alleviates the excessive consumption of land, water, biological, and other resources caused by environmental degradation
	(2) the accumulation of gangue mountain to the occupation of cultivated land resources is reduced
society	(1) it responds to the call of related green mining policy in China
	(2) it is conducive to the intelligent and efficient development of various industries in China
	(3) the harm to the physical and mental health of the local population is reduced
	(4) the social burden caused by economy and environment is alleviated

7. CONCLUSIONS

In order to ensure the balance between loss reduction mining and solid waste emission reduction in the process of top coal caving and realize clean production, this study builds a top coal caving simulation test bed and conducts coal gangue recognition research based on MS time−frequency domain fusion. Several conclusions can be drawn as follows.

(1) The way of comprehensive treatment of gangue is the realization of loss reduction mining and solid waste emission reduction, and the fundamental method is the accurate recognition of the coal gangue interface.

(2) By building a simulation test bed for top coal caving, the MS signals of a coal gangue mixture with a gangue content of 0−100% are extracted. After preprocessing, 12 time domain features such as mean, absolute mean, and standard deviation and 12 frequency domain features such as spectrum mean, frequency variance, and frequency center of gravity of each signal are extracted.

(3) Two feature fusion methods, OTFDF-FM and TFDFS-FM, are proposed. By comparison, the recognition accuracy of the TFDFS-FM is higher, reaching 98.8% when using all sensor signals.

(4) The fusion frequency of each feature in the process of TFDF selection fusion is studied, and it is found that the sensitivity ranking of features is different when fusing different sensor signals. Therefore, each data set has its corresponding optimal feature subset.

(5) Through the processing of TFDFS-FM and the MS signal fusion method, the recognition accuracy of the sample set can be improved to 99% under the AdaBoost algorithm when six sensors are fused. While ensuring high-precision recognition, the number of sensors and features is reduced.

The results of this paper prove the recognition ability of the MS-TFDF-F-based coal gangue recognition model. This research lays the foundation for accurately defining the coal−

gangue interface and realizing the balance between loss reduction mining and solid waste emission reduction in the process of top coal caving, which is of great significance to promote the clean and green development of the coal mining industry. In this paper, only the accuracy of the coal gangue recognition model is considered, while the response speed is not studied. It will be the future development direction to establish a multi-index and comprehensive coal gangue recognition model.

With the development of China's industrialization, people's demand for energy is rising, however, we should always uphold people-oriented thinking. The environment in which human beings live, the economy they develop, the resources they rely on, and the society they live in should be placed within the scope of resource development priorities.

■ AUTHOR INFORMATION

Corresponding Authors

Yang Yang − *College of Mechanical and Electrical Engineering, Shandong University of Science and Technology, Qingdao 266590, China;* ● orcid.org/0000-0001-6304-6362; Email: yang.yang@sdust.edu.cn, sdkdyangyang@126.com

Qingliang Zeng − *College of Mechanical and Electrical Engineering, Shandong University of Science and Technology, Qingdao 266590, China;* Email: sdkdsdustqlzeng@126.com

Author

Yao Zhang − *College of Mechanical and Electrical Engineering, Shandong University of Science and Technology, Qingdao 266590, China*

Complete contact information is available at:
https://pubs.acs.org/10.1021/acsomega.3c02319

Author Contributions

[†]Y.Z. and Y.Y. contributed to the work equally and should be regarded as co-first authors.

Notes

The authors declare no competing financial interest.

■ ACKNOWLEDGMENTS

■ REFERENCES

(1) Li, Y.; Zhang, C.; Tang, D.; Gan, Q.; Niu, X.; Wang, K.; Shen, R. Coal pore size distributions controlled by the coalification process: An experimental study of coals from the Junggar, Ordos and Qinshui basins in China. *Fuel* **2017**, *206*, 352−363.

(2) Wang, J. 40 years development and prospect of longwall top coal caving in China. *J. China Coal Soc.* **2023**, *48* (01), 83−99.

(3) Zhang, J.; Liu, X.; Liu, Y.; Shao, X. p.; Zhang, H. m. Study of Top Coal Partition and Key Delayed-Action Region for Horizontal Sublevel Top Coal Caving in Deeply Inclined Seam. *Math. Probl. Eng.* **2021**, *2021*, 1−10.

(4) Wang, S.; Liu, L.; Zhao, Y.; Zhang, B. New energy exploitation in coal occurrence under the target of "Double Carbon"—a new path for transformation and upgrading coal mines in the future. *Coal Sci. Technol.* **2023**, *51* (01), 59−79.

(5) Yang, S.; Xu, Y.; Kang, H.; Li, K.; Li, C. Investigation into starch adsorption on hematite and quartz in flotation: role of starch molecular structure. *Appl. Surf. Sci.* **2023**, *623*, 157064.

(6) Wang, Q.; Zhang, H.; Xu, Y.; Bao, S.; Liu, C.; Yang, S. The molecular structure effects of starches and starch phosphates in the reverse flotation of quartz from hematite. *Carbohydr. Polym.* **2023**, *303*, 120484.

(7) Zhu, X.; Huang, Y.; Zhu, Y.; Sun, N.; Wang, W. Investigating the performance of oxalic acid for separating bastnaesite from calcium-bearing gangue minerals based on experiment and theoretical calculation. *Miner. Eng.* **2021**, *170*, 107047.

(8) Yan, Y.; Yang, C.; Peng, L.; Li, R.; Bai, H. Emission characteristics of volatile organic compounds from coal-coal,gangue- and biomass-fired power plants in China. *Atmos. Environ.* **2016**, *143*, 261−269.

(9) Chen, L.; Li, J.; Zhang, D.; Fan, G.; Zhang, W.; Guo, Y. Microscopic fabric evolution and macroscopic deformation response of gangue solid waste filler considering block shape under different confining pressures. *Sci. Rep.* **2022**, *12*, 7388.

(10) Vo, T. L.; Nash, W.; Del Galdo, M.; Rezania, M.; Crane, R.; Mousavi Nezhad, M.; Ferrara, L. Coal mining wastes valorization as raw geomaterials in construction: A review with new perspectives. *J. Cleaner Prod.* **2022**, *336*, 130213.

(11) Zhang, J.; Zhang, Q.; Zhou, N.; Li, M.; Huang, P.; Li, B. Research progress and prospect of coal based solid waste backfilling mining technology. *J. China Coal Soc.* **2022**, *47*, 4168−4170.

(12) Xuan, D.; Xu, J.; Wang, B. Green mining technology of overburden isolated grout injection. *J. China Coal Soc.* **2022**, *47*, 4265−4277.

(13) Dou, D.; Wu, W.; Yang, J.; Zhang, Y. Classification of coal and gangue under multiple surface conditions via machine vision and relief-SVM. *Powder Technol.* **2019**, *356*, 1024−1028.

(14) Lv, Z.; Wang, W.; Xu, Z. Cascade network for detection of coal and gangue in the production context. *Powder Technol.* **2021**, *377*, 361−371.

(15) Zhang, J.; Han, X.; Cheng, D. Improving coal gangue recognition efficiency based on liquid intervention with infrared imager at low emissivity. *Measurement* **2022**, *189*, 110445.

(16) Wang, J. C.; Pan, W.; Zhang, G.; Yang, S.; Yang, K.; Liang, L. Principles and applications of image-based recognition of withdrawn coal and intelligent control of drawing opening in longwall top coal caving face. *J. China Coal Soc.* **2022**, *47*, 87−101.

(17) Yang, Y.; Zeng, Q. Impact-slip experiments and systematic study of coal gangue "category" recognition technology Part I: Impact-slip experiments between coal gangue mixture and top coal caving hydraulic support and the study of coal gangue "category" recognition technology. *Powder Technol.* **2021**, *392*, 224−240.

(18) Yang, Y.; Zeng, Q. Impact-slip experiments and systematic study of coal gangue "category" recognition technology part II: Improving effect of the proposed parallel voting system method on coal gangue "category" recognition accuracy based on impact-slip experiments. *Powder Technol.* **2022**, *395*, 893−904.

(19) Li, Y. M.; Bai, L.; Jiang, Z. Caving coal-rock identification based on EEMD-KPCA and KL divergence. *J. China Coal Soc.* **2020**, *45*, 827−835.

(20) Pang, H.; Wang, S.; Dou, X.; Liu, H.; Chen, X.; Yang, S.; Wang, T.; Wang, S. A feature extraction method using auditory nerve response for collapsing coal-gangue recognition. *Appl. Sci.* **2020**, *10*, 7471.

(21) Yuan, Y.; Wang, J.; Zhu, D. Feature extraction and classification method of coal gangue acoustic signal during top coal caving. *J. Min. Sci. Technol.* **2021**, *6*, 711−720.

(22) Jiang, H.; Zong, D.; Song, Q.; Gao, K.; Shao, H.; Liu, Z.; Tian, J. Coal gangue recognition via multi-branch convolutional neural network based on MFCC in noisy environment. *Sci. Rep.* **2023**, *13*, 6541.

(23) Zhang, N.; Liu, C. Radiation characteristics of natural gamma-ray from coal and gangue for recognition in top coal caving. *Sci. Rep.* **2018**, *8*, 190.

(24) Liu, C.; Zhang, N.; Guo, F.; An, S.; Chen, B. Sequential rules and identification method of coal-gangue-rock caving flow in fully mechanized top-coal-caving workface of extra thick comprehensive coal seam. *J. China Coal Soc.* **2022**, *47*, 137−151.

(25) Zhang, S. X.; Zhang, X.; Liu, S. Intelligent precise control technology of fully mechanized top coal caving face. *J. China Coal Soc.* **2020**, *45*, 2008−2020.

(26) Si, L.; Tan, C.; Zhu, J. A coal gangue recognition method based on X-ray image and laser point cloud. *Chin. J. Sci. Instrum.* **2022**, *43*, 193−205.

(27) Wang, X.; Guo, Y.; Wang, S.; Cheng, G.; Wang, X.; He, L. Rapid detection of incomplete coal and gangue based on improved PSPNet. *Measurement* **2022**, *201*, 111646.

(28) Li, L.; Zhu, J.; Liu, L. Research on coal gangue recognition method based on density difference. *Coal Technol.* **2022**, *41*, 181−184.

(29) Zhang, J.; He, G.; Yang, S. Controlling water temperature for efficient coal gangue recognition. *Mater. Today Chem.* **2021**, *22*, 100587.

(30) Wang, X.; Wang, S.; Guo, Y.; Hu, K.; Wang, W. Dielectric and geometric feature extraction and recognition method of coal and gangue based on VMD-SVM. *Powder Technol.* **2021**, *392*, 241−250.

(31) Yang, Y.; Zhang, Y.; Zeng, Q. Research on coal gangue recognition based on multi-layer time domain feature processing and recognition features cross-optimal fusion. *Measurement* **2022**, *204*, 112169.

(32) Li, X.; Xu, Y.; Li, N.; Yang, B.; Lei, Y. Remaining useful life prediction with partial sensor malfunctions using deep adversarial networks. *IEEE/CAA J. Autom. Sin.* **2023**, *10*, 121−134.

(33) Huo, Y.; Zhu, D.; Wang, Z.; Song, X. Numerical Investigation of Top Coal Drawing Evolution in Longwall Top Coal Caving by the Coupled Finite Difference Method-Discrete Element Method. *Energies* **2021**, *14*, 219.

(34) Liang, M.; Hu, C.; Yu, R.; Wang, L.; Zhao, B.; Xu, Z. Optimization of the Process Parameters of Fully Mechanized Top-Coal Caving in Thick-Seam Coal Using BP Neural Networks. *Sustainability* **2022**, *14*, 1340.

(35) Zhang, L.; Shen, W.; Li, X.; Wang, Y.; Qin, Q.; Lu, X.; Xue, T. Abutment pressure distribution law and support analysis of super large mining height face. *Int. J. Environ. Res. Public Health* **2023**, *20*, 227.

(36) Li, X.; Zhang, X.; Shen, W.; Zeng, Q.; Chen, P.; Qin, Q.; Li, Z. Research on the mechanism and control technology of coal wall sloughing in the ultra-large mining height working face. *Int. J. Environ. Res. Public Health* **2023**, *20*, 868.

(37) Zhang, J.; Li, X.; Qin, Q.; Wang, Y.; Gao, X. Study on overlying strata movement patterns and mechanisms in super-large mining height stopes. *Bull. Eng. Geol. Environ.* **2023**, *82*, 142.

(38) Shen, J.; Zhang, Y. Theory and Application of Gob-Side Entry Retaining in Thick Three-Soft Coal Seam. *Geofluids* **2021**, *2021*, 1−16.

(39) Huang, Z.; Quan, S.; Hu, X.; Zhang, Y.; Gao, Y.; Ji, Y.; Qi, X.; Yin, Y. Study on the preparation and inhibition mechanism of intumescent nanogel for preventing the spontaneous combustion of coal. *Fuel* **2022**, *310*, 122240.

(40) Liu, S.; Li, X. Experimental study on the effect of cold soaking with liquid nitrogen on the coal chemical and microstructural characteristics. *Environ. Sci. Pollut. Res.* **2023**, *30*, 36080−36097.

(41) Liu, S.; Sun, H.; Zhang, D.; Yang, K.; Wang, D.; Li, X.; Long, K.; Li, Y. Nuclear magnetic resonance study on the influence of liquid nitrogen cold soaking on the pore structure of different coals. *Phys. Fluids* **2023**, *35*, 012009.

(42) Liu, S.; Sun, H.; Zhang, D.; Yang, K.; Li, X.; Wang, D.; Li, Y. Experimental study of effect of liquid nitrogen cold soaking on coal pore structure and fractal characteristics. *Energy* **2023**, *275*, 127470.

(43) Yang, K.; Zhao, X.; He, X.; Wei, Z. Basic theory and technical system of multi-source coal based solid waste green filling. *J. China Coal Soc.* **2022**, *47*, 4201−4216.

(44) Zhang, X.; Li, F.; Zhao, Q.; Li, X. Leaching characteristics and potential ecological risks of typical heavy metals in gangue. *J. China Coal Soc.* **2022**, *47*, 235−245.

(45) Hu, Z. Q.; Xiao, W.; Zhao, Y. Re-discussion on coal mine ecol-environment concurrent mining and reclamation. *J. China Coal Soc.* **2020**, *45*, 351−359.

(46) Zecevic, M.; Lebensohn, R. A.; Capolungo, L. New large-strain FFT-based formulation and its application to model strain localization in nano-metallic laminates and other strongly anisotropic crystalline materials. *Mech. Mater.* **2022**, *166*, 104208.

(47) Xiang, C.; Ren, Z.; Shi, P.; Zhao, H. Data-Driven Fault Diagnosis for Rolling Bearing Based on DIT-FFT and XGBoost. *Complexity* **2021**, *2021*, 1−13.

(48) Sharma, L.; Peerlings, R.; Geers, M.; Roters, F. Integral nonlocal approach to model interface decohesion in FFT solvers. *Eng. Fract. Mech.* **2021**, *243*, 107516.

(49) Li, W.; Suhayb, M.; Thangavelu, L.; Abdulameer Marhoon, H.; Pustokhina, I.; Alqsair, U. F.; El-Shafay, A.; Alashwal, M. Implementation of AdaBoost and genetic algorithm machine learning models in prediction of adsorption capacity of nanocomposite materials. *J. Mol. Liq.* **2022**, *350*, 118527.

(50) Liu, G.; Tsai, S. B. A Study on the Design and Implementation of an Improved AdaBoost Optimization Mathematical Algorithm Based on Recognition of Packaging Bottles. *Math. Probl. Eng.* **2022**, *2022*, 1−11.

(51) Sevinç, E. An empowered AdaBoost algorithm implementation: A COVID-19 dataset study. *Comput. Ind. Eng.* **2022**, *165*, 107912.